RSC Advances

This article can be cited before page numbers have been issued, to do this please use: L. Bie, X. Luo, Q. He, D. He, Y. Liu and P. Jiang, *RSC Adv.*, 2016, DOI: 10.1039/C6RA19576H.

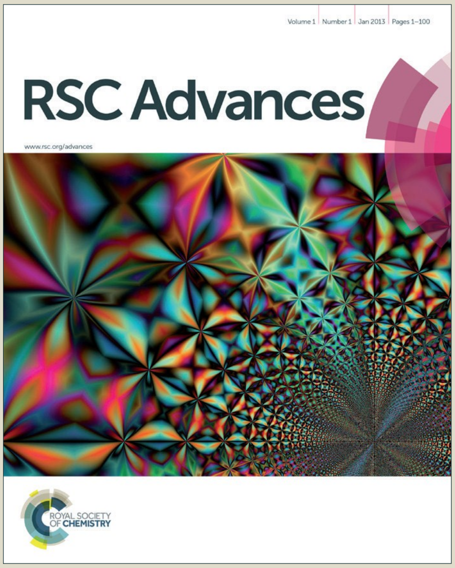

ROYAL SOCIETY
OF CHEMISTRY

www.rsc.org/advances

Journal Name

Dynamic Article Links ▶
View Article Online
DOI: 10.1039/C6RA19576H

Cite this: DOI: 10.1039/c0xx00000x

www.rsc.org/xxxxxx

ARTICLE TYPE

Hierarchical Cu/Cu(OH)$_2$ nanorod arrays grown on Cu foam as a high-performance 3D self-supported electrode for enzyme-free glucose sensing

Lili Bie, Xue Luo, Qingqing He, Daiping He, Yan Liu and Ping Jiang*

Received (in XXX, XXX) Xth XXXXXXXXX 20XX, Accepted Xth XXXXXXXXX 20XX
DOI: 10.1039/b000000x

Hierarchical Cu/Cu(OH)$_2$ nanorod arrays grown on commercially available Cu foam (Cu/Cu(OH)$_2$ NRA/CF) was prepared via a three-step strategy involving the wet chemical synthesis of Cu(OH)$_2$ NRA/CF, chemical reduction reaction for conversion from Cu(OH)$_2$ NRA/CF to Cu NRA/CF, and finally galvanostatic anodization to grow Cu(OH)$_2$ nanoparticles on Cu NRA/CF. Hierarchical Cu/Cu(OH)$_2$ NRA/CF shows highly catalytic activity towards glucose oxidation in an alkaline solution and be served as a promising electrode material for enzyme-free glucose sensing. At an applied potential of + 0.5 V, the sensor showed a broad detection range of 0.001-1.0 mM, a high sensitivity of 9.18 mA mM^{-1} cm^{-2}, and a low detection limit of 0.45 μM (S/N = 3). Furthermore, the sensor exhibits excellent selectivity against the common interferences and good reliability for glucose detection in human serum samples.

Introduction

Numerous efforts have been devoted to glucose detection because of its wide application in biotechnology, clinical diagnostics, food industry and many other fields.[1,2] Electrochemical methods have been widely investigated and utilized due to its remarkable features such as high sensitivity, super selectivity, simple instrumentation, and easy operation.[3] In past decades, enzymatic glucose electrochemical sensors have attracted extensive attention for their high sensitivity and selectivity towards glucose oxidation. However, such sensors often suffer from high cost, time-consuming operation and insufficient long-term stability originating from the intrinsic nature of enzymes.[3,4] Electrochemical enzyme-free glucose sensors based on the direct electrochemical oxidation of glucose triggered great interest and were widely exploited.[5,6] Noble metals[7-9] and their composites[10,11] were exploited as electrode materials for enzyme-free glucose sensing in the early research studies, but most of them have distinct problems including low sensitivity and poor selectivity resulted from the surface poisoning effects, as well as high cost and limited reserves. Therefore, tremendous efforts are focused on fabricating high-performance sensors using low-cost and earth-abundant metals, such as copper, [12,13] cobalt,[14,15] nickel,[16,17] and so on.

Hierarchical nanostructured architectures[18-20] self-assembled from low-dimensional nanostructured building blocks have become a class of significant functional materials. Due to their larger surface, good conductivity and permeability, hierarchical nanomaterials arouse much interest in many emerging research fields, especially environmental remediation, sensor, and energy conversion. Various hierarchical nanostructures such as hyper-branched Cu@Cu$_2$O coaxial nanowires, [21] hierarchical Ni/NiO core-shells nanostructure[22] and 3D hierarchical cobalt oxide architecture,[23] have been demonstrated as novel electrode materials for glucose sensing with high sensitivity and good selectivity. For electrochemical tests, however, it requires the effective immobilization of these hierarchical nanomaterials on electrode surfaces with the use of polymer binder (Nafion or PTFE) as a film-forming agent. The whole process is time-consuming and such polymer binder may block the active sites of the catalyst, inhibit the diffusion of analyte, and increase the series resistance of the device, leading to reduced catalytic activity.[24,25] As a result, it is of significant importance to prepare self-supported electrode by directly growing hierarchical nanostructures on conductive substrate.[26-29]

Metal foam such as Cu foam [30,31] and Ni foam[26,32], as a commercial available material with 3D porous structure and excellent electrical conductivity, has been used extensively as an efficient conductive substrate for constructing various self-supported electrodes. Due to the unique pore structure and large surface area, metal foam not only facilitates sufficient transport of reactants and products in electrochemical process, but also provides more catalyst loading and more active sites exposure, leading to an improved catalytic activity.

In this paper, we demonstrated the successful synthesis of hierarchical Cu/Cu(OH)$_2$ nanorod arrays supported on Cu foam (Cu/Cu(OH)$_2$ NRA/CF) via a three-step strategy. Firstly, Cu(OH)$_2$ nanorod arrays grown on Cu foam (Cu(OH)$_2$ NRA/CF) were fabricated by a simple wet chemical reaction.

Key Laboratory of Green Synthesis and Applications, College of Chemistry, Chongqing Normal University, Chongqing 401331, China. Corresponding author, E-mail: jphdp868@126.com

† Electronic Supplementary Information (SI) available: Experimental section and Figures. See DOI:

View Article Online
DOI: 10.1039/C6RA19576H

The $Cu(OH)_2$ NRA/CF were subsequently converted to Cu nanorod arrays on Cu foam (Cu NRA/CF) by a $NaBH_4$ reduction reaction. Finally, galvanostatic anodization of corresponding Cu NRA/CF produces hierarchical $Cu/Cu(OH)_2$ NRA/CF. As a novel self-supported electrode for enzyme-free glucose sensing, the presented $Cu/Cu(OH)_2$ NRA/CF exhibits superior catalytic activity than other sensors including $Cu(OH)_2$ NRA grown on conductive substrate, commercial Cu foam, $Cu/Cu(OH)_2$ NRA grown on Cu foil ($Cu/Cu(OH)_2$ NRA/CFL), and various other hierarchical nanostructured glucose sensors. The high performance of $Cu/Cu(OH)_2$ NRA/CF can be attributed to the following reasons: (1) The 3D CF used as conductive substrate with a large surface area leads to a significant increase in the catalyst loading and more active site exposure. (2) Hierarchical structure of $Cu/Cu(OH)_2$ NRA owns large specific surface area, facilitating more active site exposure. (3) The direct growth of $Cu/Cu(OH)_2$ NRA on CF enables intimate contact, good adhesion and excellent electrical connection between them.[33] Moreover, the absence of a polymer binder avoids the blocking of active site[24] and the inhibition of diffusion.[25]

Experimental section

Materials

CF was purchased from Aladdin Ltd. (Shanghai, China). Ethanol, acetone, HCl, $(NH_4)_2S_2O_8$, NaOH, $NaBH_4$ and KOH were bought from Chengdu Chemical Reagent Factory (Chengdu, China). Ascorbic acid (AA), uric acid (UA), dopamine (DA) and d-(+)-glucose were supplied by J&k Chemical Ltd. (China). Human serum was supplied by Chongqing Emergency Medical Central. All aqueous solutions were prepared with deionized water.

Preparation of $Cu(OH)_2$ NRA/CF

Prior to wet chemical reaction, a piece of CF (2 cm × 2 cm) was washed with ethanol, acetone, 3 M HCl and water respectively to remove the surface impurities and dried in air. The cleaned CF was then immersed in an aqueous solution including 2 M NaOH and 1 M $(NH_4)_2S_2O_8$ (mole ratio is 20:1) for 1 h at room temperature. The resulted $Cu(OH)_2$ NRA/CF was removed from the solution and washed with water several times, then dried in air.

Preparation of Cu NRA/CF

Cu NRA/CF were prepared by immersing the corresponding $Cu(OH)_2$ NRA/CF in 1 M $NaBH_4$ aqueous solution for at least 20 min, then was washed with water and dried in a vacuum over at 80 □ for 2 h.

Preparation of $Cu/Cu(OH)_2$ NRA/CF

$Cu/Cu(OH)_2$ NRA/CF were obtained by galvanostatic anodization of the resulted Cu NRA/CF in an alkaline solution (3 M KOH) for 200 s, with current density kept at 10 mA/cm^2.

Preparation of $Cu/Cu(OH)_2$ NRA/CFL

$Cu/Cu(OH)_2$ NRA/CFL were prepared with the same method except that a piece of Cu foil was used as a conductive substrate.

Characterizations

Powder XRD data were acquired on a RigakuD/MAX 2550 diffractometer with Cu Kα radiation (λ=1.5418 Å). SEM measurements were carried out on a XL30 ESEM FEG scanning electron microscope at an accelerating voltage of 20 kV. All electrochemical measurements were performed on a Autolab PGSTAT 302 electrochemical workstation (Metrohm Ltd, Switzerland). A typical three-electrode system was employed with a saturated Ag/AgCl as reference electrode, a Pt wire as counter electrode, and the $Cu/Cu(OH)_2$ NRA/CF (0.5 cm × 0.5 cm) as a working electrode. All electrochemical experiments were performed at room temperature and all the potentials are reported against the saturated Ag/AgCl reference electrode. For amperometric detection, all measurements were performed by applying an appropriate potential to the working electrode and allowing the transient background current to decay to a steady-state value before the addition of the analyte. The solution was stirred to provide convective transport.

Results and discussion

Scheme 1 represents the formation of the hierarchical $Cu/Cu(OH)_2$ NRA/CF and its application for glucose sensing. As is shown, three-step synthesis process was involved in the preparation of hierarchical nanostructures. According to the previous reports,[34] $Cu(OH)_2$ NRA/CF was firstly prepared by simply immersing CF in an aqueous solution containing NaOH and $(NH_4)_2S_2O_8$. Then, the resulted $Cu(OH)_2$ NRA/CF was reduced to metallic Cu NRA/CF with putting $Cu(OH)_2$ NRA/CF into 1 M $NaBH_4$ aqueous solution for at least 20 min. After being washed with deionized water and dried in a vacuum oven at 80□ for 2 h, the Cu NRA/CF was subsequently put in an alkaline solution for galvanostatic anodization, with the current density kept at 10 mA/cm^2. After that, the $Cu/Cu(OH)_2$ NRA/CF with hierarchical structure was obtained.

Fig. 1 shows the X-ray diffraction (XRD) patterns for $Cu(OH)_2$ NRA/CF (curve a), Cu NRA/CF (curve b) and $Cu/Cu(OH)_2$ NRA/CF (curve c), respectively. Curve a shows diffraction peaks indexed to orthorhombic phase $Cu(OH)_2$ (JCPDS No.72-0140)[34] and that of metallic copper (JCPDS No. 04-0836)[35] originated from CF, suggesting successfully synthesis of $Cu(OH)_2$ NRA grown on Cu foam by wet chemical method. After chemical reduction with $NaBH_4$ solution, only the diffraction peaks (curve b) of the copper are observed at 43.3°, 50.4° and 74.1°, which are well indexed to (111), (200) and (220) planes of metallic Cu (JCPDS No. 04-0836), implying the complete reduction of $Cu(OH)_2$ NRA. Following galvanostatic anodization, the diffraction peaks (curve c) indexed to $Cu(OH)_2$ (JCPDS No.72-0140) appears again, indicating that galvanostatic anodization cause the growth of $Cu(OH)_2$ on Cu NRA/CF.

Fig. 2a shows SEM images of $Cu(OH)_2$ NRA/CF in low-magnification, indicating they are 1D structures about several micrometers in length. The high-magnification SEM image (see Fig. 2b) further reveals that they have diameters ranging from 100 nm to 200 nm with smooth surface. After chemical reduction

View Article Online
DOI: 10.1039/C6RA19576H

with $NaBH_4$ solution, such $Cu(OH)_2$ NRA were found converted to Cu NRA with diameter less than 100 nm, rough surface and decreased length (Fig 2c and 2d). The development of such morphology is associated with hydrogen release and conversion from $Cu(OH)_2$ to metallic Cu. Galvanostatic anodizing Cu NRA in an alkaline solution for 200 s produces a large quantity of uniform nanoparticles with diameter around 50 nm grown on its surface (Fig. 2e and 2f), constructing a hierarchical structure consisted by one-dimensional nanorods and zero-dimensional nanoparticles. XRD patterns in Fig. 1 confirmed the composition of these nanostructures. All results suggests the successful fabrication of hierarchical structure of Cu/$Cu(OH)_2$ NRA/CF.

Nitrogen adsorption-desorption isotherm measurement (Fig S1) was conducted to investigate the surface areas of the as prepared Cu/$Cu(OH)_2$ NRA scratched down from the Cu foil. The Brunauer-Emmett-Teller (BET) specific surface area (SSA) of Cu/$Cu(OH)_2$ NRA was calculated to be 27.60 m^2/g, much larger than that of Cu NRA (12.25 m^2/g), which can be attributed to its hierarchical structure.

Electrochemical impedance spectrum (EIS) is an effective way to measure the electron transfer resistance. Fig. 3a shows the typical EIS of the CF, $Cu(OH)_2$ NRA/CF, Cu NRA/CF, and Cu/$Cu(OH)_2$ NRA/CF. As for bare Cu foam, a small semicircular portion at high frequency is observed, illustrating low transfer resistance and good conductivity of the CF. After being covered with $Cu(OH)_2$ NRA, the semicircle diameter was observed increases from a value close to 30 ohm up to 110 ohm, implying inferior conductivity of $Cu(OH)_2$. However, it returns to a value about 25 ohm after the complete conversion from $Cu(OH)_2$ NRA/CF to Cu NRA/CF. Compared with the bare CF, Cu NRA/CF shows lower transfer resistance which can be attributed to the superior conductivity of Cu nanostructure. After the growth of $Cu(OH)_2$ nanoparticles on the surface of Cu NRA, the semicircle diameter has a slight increase but still keeps smaller than that of $Cu(OH)_2$ NRA/CF, implying superior conductivity and faster electron transfer of the hierarchical Cu/$Cu(OH)_2$ NRA/CF.

The electrochemical behavior of Cu/$Cu(OH)_2$ NRA/CF was examined in 0.1 M NaOH solution (Fig. 3b). For comparison, CF and Cu/$Cu(OH)_2$ NRA/CFL were also examined. Like any other Cu based nanomaterials,[31,36,37] the oxidative current of Cu(II) to Cu(III) in the potential range +0.4 V to + 0.7 V was not clear. However, the cathodic peak at about + 0.57 V, corresponding to the reduction of Cu(III) to Cu(II), was observed on reversing the scan, clearly indicating the presence of Cu(III).[38]. Here, we compared the cyclic voltammograms (CVs) behaviors of three kinds of Cu based electrodes. As is shown, bare CF exhibits lower current response while Cu/$Cu(OH)_2$ NRA grown on both CF and CFL show higher amperometric responses, which should be attributed to the larger specific surface area of the Cu/$Cu(OH)_2$ NRA originated from its hierarchical nanostructure. Due to the pore structure, CF owns larger specific surface and benefits more Cu/$Cu(OH)_2$ NRA loading and more active sites exposure. Consequently, Cu/$Cu(OH)_2$ NRA/CF exhibits larger current responses than that of Cu/$Cu(OH)_2$ NRA/CFL in the same conditions.

The electrocatalytic activity of Cu/$Cu(OH)_2$ NRA/CF towards glucose oxidation in an alkaline solution was also investigated. Fig. 4a shows the CVs of Cu/$Cu(OH)_2$ NRA/CF electrode in the absence (black curve) and presence (red curve) of 1.0 mM glucose in 0.1 M NaOH solution. No obvious oxidation peak was observed in absence of glucose. However, a gradual increase in anodic current was observed at + 0.5 V when the glucose was added, followed a slight decrease in cathodic current, indicative of an irreversible electro-oxidation reaction that occurred at approximately + 0.5 V during scanning.[31] According to the previous research, the enhanced anodic current is attributed to the electrochemical oxidation of glucose with the participation of Cu(III).[39,40] The possible mechanism of the electrocatalytic process of glucose can be expressed as followings:[38]

$$Cu(II) + OH^{-} \rightarrow Cu(III) + e^{-}$$

$$Cu(III) + glu\cos e \rightarrow Cu(II) + gluconolactone$$

Fig. 4b shows the CVs curves of Cu/$Cu(OH)_2$ NRA/CF in 0.1 M NaOH solution including 0.1 mM glucose at different scan rates. The anodic peak current of oxidation of glucose (the corresponding voltage is at + 0.5 V) was found proportional to the scan rate. As indicated in the inset of Fig 4b, a good linearity between scan rate and perk current within the range of 1-50 mV/s was observed, indicating a surface-controlled electrochemical kinetic process of Cu/$Cu(OH)_2$ NRA/CF in alkaline solution.

The optimal operating potential for electrochemical detecting glucose with Cu/$Cu(OH)_2$ NRA/CF was further studied. Fig. 5 shows the amperometric responses towards dropwise addition of 0.01 mM glucose into 0.1 M NaOH solution at different potentials. A well-defined, stable and rapid change in current can be observed with the successive additions of 0.01 mM glucose under detection potentials from 0.40 V to 0.55 V in 0.05 V increments. The Cu/$Cu(OH)_2$ NRA/CF exhibits sensitive and rapid current response to the glucose addition, achieving steady state current in less than 5 s. The sensitivity is enhanced steadily in the range from 0.40 to 0.50 V. However, a slight decrease is observed when the potential beyond 0.55 V. Therefore, the followed amperometric detection of glucose was performed under the potential of 0.50 V.

Fig. 6a shows an amperometric response of Cu/$Cu(OH)_2$ NRA/CF with successive addition of the glucose solution with different concentrations into 0.1 M NaOH solution, at an applied potential of 0.50 V. The addition of glucose was incremented at the rate of 1, 5, 10, 50, 100 and 500 μM, respectively. As shown in Fig 6b, the Cu/$Cu(OH)_2$ NRA/CF gives a linear dependence range from 1μM to 1 mM of glucose with a correlation coefficient (R^2) of 0.991 and a remarkably high sensitivity of 9.18 mA mM^{-1} cm^{-2}. Such sensitivity is better than those of 418 μA mM^{-1} cm^{-2} at $Cu(OH)_2$ nanotube arrays[38] on copper foils, and 5.85 mA mM^{-1} cm^{-2} at commercial Cu foam.[41] Moreover, compared with other copper-based enzyme-free glucose sensors with hierarchical nanostructure (Tab S2), the sensitivity is still better than those of 1.321 mA mM^{-1} cm^{-2} at CuO/TiO_2 nanocomposites,[42] 2.657 mA mM^{-1} cm^{-2} at hierarchical CuO nanoflowers,[43] 1.42 mA mM^{-1} cm^{-2} at hyper-branched Cu@Cu_2O coaxial nanowires,[21] 0.408 mA mM^{-1} cm^{-2} at CuO/ZnO hybrid hierarchical nanostructures,[44] 3.252 mA

View Article Online
DOI: 10.1039/C6RA19576H

mM^{-1} cm^{-2} at chrysanthemum-like CuO hierarchical film,[36] 4.078 mA mM^{-1} cm^{-2} at candock-like CuO hierarchical film,[36] 5.368 mA mM^{-1} cm^{-2} at dandelion-like CuO hierarchical film,[36] and 3.36 mA mM^{-1} cm^{-2} at $Cu(OH)_2$ nanorods decorated porous graphene foam ($Cu(OH)_2$ /PGF).[45] The superior sensitivity for Cu/$Cu(OH)_2$ NRA/CF can be attributed to the following three reasons: (1) The porous feature for CF not only favors more catalyst loading and more active sites exposure, but allows more easy diffusion of electrolyte and faster electron transfer in process of electrochemistry. (2) The hierarchical structure of Cu/$Cu(OH)_2$ NRA also facilitates the exposure of more active sites during the electrocatalytic process. (3) The direct growth of Cu/$Cu(OH)_2$ NRA on CF avoids the use of polymer binder, thus effectively decreases the contact electrical resistance between them and benefits more active site exposure.

The response time was found less than 5 s to reach 95% of steady-state current from the enlarged segment of the amperometric response curve (inset in Fig. 6a) and the limit of detection (LOD) was found to be 0.45 μM based on signal-to-noise ratio of 3. The detection limit of the as-prepared Cu/$Cu(OH)_2$ NRA/CF is relatively low among other hierarchical Cu based nanostructures (Tab S1), implying high performance towards glucose sensing.

It is well known that some easily oxidative species such as dopamine (DA), ascorbic acid (AA), and uric acid (UA), usually co-exist with glucose in biological sample and consequently interfere with the detection of glucose. Therefore, anti-interference property is another important parameter for the practical use of glucose sensors. Herein, the interference test was also investigated using Cu/$Cu(OH)_2$ NRA/CF to evaluate the possible application in glucose detection in human serum. Since the normal physiological level of glucose (3-8 mM) is more than 10 times higher higher than those of the other three interfering species, [46] the molar ratio of 10:1 was used for AA, UA, and DA to estimate their interference effects in the glucose sensing. Fig. 7a shows the amperometric response of the Cu/$Cu(OH)_2$ NRA/CF for 0.1 mM glucose at 0.5 V, followed by the additions of 0.01 mM UA, 0.01 mM DA and 0.01 mM AA in a 0.1 M NaOH solution. Obviously, almost no current response for such electroactive interfering species was detected in comparison to that of glucose, indicating the high selectivity of our present Cu/$Cu(OH)_2$ NRA/CF based sensor for glucose detection in comparison to the normally co-existing electroactive interfering species.

We further evaluated the reliability of the Cu/$Cu(OH)_2$ NRA/CF sensor by detecting the concentration of glucose in human serum samples. All serum samples were supplied by Chongqing Emergency Medical Central. Fig. 7b shows the amperometric responses of the Cu/$Cu(OH)_2$ NRA/CF sensor upon addition of 5 μM glucose and three human serum samples at an applied potential of 0.5 V in 0.1 M NaOH solution. The determination of each sample was done three times to verify the reproducibility of the values. The concentration of glucose was determined by comparing the amperometric response of 5 μM glucose and that of human serum sample. Table 1. lists the glucose concentrations in serum samples obtained by the Cu/$Cu(OH)_2$ NRA/CF sensor and those measured by the hospital. The relative standard deviations (RSD) and bias are less than 3% and 0.15 mM, respectively. Obviously, the Cu/$Cu(OH)_2$ NRA/CF is suitable for glucose detection in human serum.

For practical applications, the sensors should have the advantage of good reproducibility and long-term stability. Therefore, we further probed the reproducibility and stability of the Cu/$Cu(OH)_2$ NRA/CF sensor in our experiments with the amperometric method. The reproducibility was evaluated by the measurements of the response currents towards 0.2 mM glucose in 0.1 M NaOH solution at the Cu/$Cu(OH)_2$ NRA/CF sensor. The results of five parallel experiments show that the Cu/$Cu(OH)_2$ NRA/CF sensor has good reproducibility (RSD = 2.72 %, n = 5). Moreover, the above-mentioned results obtained from human samples (Table 1) also confirm the good reproducibility of present sensor.

The long-term stability of the Cu/$Cu(OH)_2$ NRA/CF sensor was examined by measuring the amperometric response currents towards 0.01 mM glucose in 0.1 M NaOH solution. As shown in Fig S2, the current response was found maintained 80% of the original value after a month conservation at room temperature, suggesting the good long-term stability of the Cu/$Cu(OH)_2$ NRA/CF sensor.

Conclusions

Hierarchical Cu/$Cu(OH)_2$ NRA/CF was fabricated via a three-step strategy involving the wet chemical synthesis, chemical reduction and galvanostatic anodization. Benefiting from the porous substrate, hierarchical nanostructures, and self-supported property, the present Cu/$Cu(OH)_2$ NRA/CF shows remarkable catalytic activity towards glucose sensing with a high sensitivity and low detection limit. Moreover, the sensor shows high selectivity, good reproducibility and long-term stability, and good reliability for glucose detection in human samples. All these make Cu/$Cu(OH)_2$ NRA/CF a good candidate for the construction of enzyme-free glucose sensor with high-performance.

Acknowledgements

This work was supported by the Natural Science Foundation of China (21601022), the Foundation and Cutting-edge Research Plan of Chongqing (cstc2015jcyjA90002, cstc2016shmszx20004), Project of International Science and Technology Cooperation Base Construction in Chongqing (cstc2014gjhz20002), and Chongqing Education Commission (KJ110604, KJ130642).

Notes and references

1 V. Scognamiglio, Biosens. Bioelectron. 2013, **47**, 12-25.
2 C. Chen, Q. Xie, D. Yang, H. Xiao, Y. Fu, Y. Tan and S. Yao, Rsc Advances. 2013, **3**, 4473-4491.
3 Y. Song, K. Qu, C. Zhao, J. Ren and X. Qu, Adv. Mater. 2010, **22**, 2206-2210.
4 G. Rocchitta, O. Secchi, M. D. Alvau, D. Farina, G. Bazzu, G. Calia, R. Migheli, M. S. Desole, R. D. O'Neill and P. A. Serra, Anal. Chem. 2013, **85**, 10282-10288.
5 M. M. Rahman, A. J. S. Ahammad, J. H. Jin, S. J. Ahn and J. J. Lee, Sensors. 2010, **10**, 4855-4866.

DOI: 10.1039/C6RA19576H

6 Z. Zhu, L. Garcia-Gancedo, A. J.Flewitt, H. Xie, F. Moussy and W. I. Milne, Sensors. 2012, **12,** 5996-6022.

7 Y. Li, Y. Y. Song, C. Yang and X. H. Xia, Electrochem. Commun. 2007, **9**, 981-988.

8 L. Meng, J. Jin, G. Yang, T. Lu, H. Zhang and C. Cai, Anal. Chem. 2009, **81**, 7271-7280.

9 S. Park, T. D. Chung, H. C. Kim, Anal. Chem. 2003, **75**, 3046-3049.

10 H. F. Cui, J. S. Ye, X. Liu, W. D. Zhang and F. S. Sheu, Nanotechnology. 2006, **17**, 2334-2339.

11 F. Xiao, F. Zhao, D. Mei, Z. Mo and B. Zeng, Biosens. Bioelectron. 2009, **24**, 3481-3486.

12 R. Ahmad, M. Vaseem, N. Tripathy and Y. B. Hahn, Anal. Chem. 2013, **85**, 10448-10454.

13 F. Cao and J. Gong, Anal. Chim. Acta. 2012, **723**, 39-44.

14 H. Liu, X. Lu, D. Xiao, M. Zhou, D. Xu, L. Sun and Y. Song, Anal. Methods. 2013, **5**, 6360-6367.

15 H. Guan, C. Shao, S. Wen, B. Chen, J. Gong and X. Yang, Mater. Chem. Phys. 2003, **82**, 1002-1006.

16 H. Nie, Z. Yao, X. Zhou, Z. Yang and S. Huang, Biosens. Bioelectron. 2011, **30**, 28-34.

17 Y. Mu, D. Jia, Y. He, Y. Miao, H. L. Wu, Biosens. Bioelectron. 2011, **26**, 2948-2952.

18 K. Ariga, Q. Ji, M. J. McShane, Y. M. Lvov, A. Vinu and J. P. Hill, Chem. Mater. 2011, **24**, 728-737.

19 Z. Lu, W. Xu, W. Zhu, Q. Yang, X. Lei, J. Liu, Y. Li, X. Sun and X. Duan, Chem. Commun. 2014, **50**, 6479-6482.

20 N. Cheng, Y. Xue, Q. Liu, J. Tian, L. Zhang, A. M. Asiri and X. Sun, Electrochim. Acta. 2015, **163**, 102-106.

21 Y. Zhao, L. Fan, Y. Zhang, H. Zhao, X. Li, Y. Li, L. Wen, Z. Yan and Z. Huo, ACS Appl. Mater. Inter. 2015, **7**, 16802-16812.

22 C. Zhang, L. Qian, K. Zhang, S. Yuan, J. Xiao and S. Wang, J. Mater. Chem A. 2015, **3**, 10519-10525.

23 L. Han, D. Yang and A. Liu, Biosens. Bioelectron. 2015, **63**, 145-152.

24 Y. Luo, J. Jiang, W. Zhou, H. Yang, J. Luo, X. Qi, H. Zhang, Y. W. Denis, C. M. Li and T. Yu, J. Mater. Chem. 2012, **22**, 8634-8640.

25 J. D. Roy-Mayhew, G. Boschloo, A. Hagfeldt and I. A. Aksay, ACS Appl. Mater. Inter. 2012, **4**, 2794-2800.

26 L. Wang, Y. Xie, C. Wei, X. Lu, X. Li and Y. Song, Electrochim. Acta. 2015, **174**, 846-852.

27 P. Kannan, T. Maiyalagan, E. Marsili, S. Ghosh, J. Niedziolka-Jönsson and M. Jönsson-Niedziolka,. Nanoscale. 2016, **8**, 843-855.

28 L. Zhang, C. Yang, G. Zhao, J. Mu and Y. Wang, Sens. Actuators B: Chem. 2015, **210**, 190-196.

29 J. Yang, M. Cho and Y. Lee, Sens. Actuators B: Chem. 2016, **222**, 674-681.

30 J. Tian, Q. Liu, N. Cheng, A. M. Asiri and X. Sun, Angew. Chem. Int. Ed. 2014, **53**, 9577-9581.

31 X. Niu, Y. Li, J. Tang, Y. Hu, H. Zhao and M. Lan, Biosens. Bioelectron. 2014, **51**, 22-28.

32 K. Xiong, L. Li, L. Zhang, W. Ding, L. Peng, Y. Wang, S. Chen, S. Tan and Z. Wei, J. Mater. Chem A. 2015, **3**, 1863-1867.

33 J. Tian, Q. Liu, N. Cheng, A. M. Asiri and X. Sun, Angew. Chem. Int. Ed. 2014, **53**, 9577-9581.

34 Y. J. Yang, W. Li and X. Chen, J. Solid. State. Electr. 2012, **16**, 2877-2881.

35 Z. Zhuang, X. Su, H. Yuan, Q. Sun, D. Xiao and M. M. F. Choi, Analyst 2008, **133**, 126-132.

36 K. Li, G. Fan, L. Yang and F. Li, Sens. Actuators B: Chem. 2014, **199**, 175-182.

37 S. Sun, Y. Sun, A. Chen, X. Zhang and Z. Yang, Analyst 2015, **140**, 5205-5215.

38 S. Zhou, X. Feng, H. Shi, J. Chen, F. Zhang and W. Song, Sens. Actuators B: Chem. 2013, **177**, 445-452.

39 L. Qian, J. Mao, X. Tian, H. Yuan and D. Xiao, Sens. Actuators B: Chem. 2013, **176**, 952-959.

40 J. Luo, S. Jiang, H. Zhang, J. Jiang and X. Liu, Anal. Chim. Acta. 2012, **709**, 47-53.

41 L. Bie, X. Luo, L. Kang, D. He and P. Jiang, Electroanalysis. 2016, **28**, 2070-2074.

42 J. Chen, L. Xu, R. Xing, J. Song, H. Song, D. Liu and J. Zhou,. Electrochem. Commun. 2012, **20**, 75-78.

43 S. Sun, X. Zhang, Y. Sun, S. Yang, X. Song and Z. Yang, Phys. Chem. Chem. Phys. 2013, **15**, 10904-10913.

44 S. SoYoon, A. Ramadoss, B. Saravanakumar and S. J. Kim, J. Electroanal. Chem. 2014, **717**, 90-95.

45 I. Shackery, U. Patil, A. Pezeshki, N. M. Shinde, S. Kang, S. Im and S. C. Jun, Electrochim. Acta. 2016, **191**, 954-961.

46 E. Scavetta, B. Ballarin and D. Tonelli, Electroanalysis. 2010, **22**, 427-432.

View Article Online
DOI: 10.1039/C6RA19576H

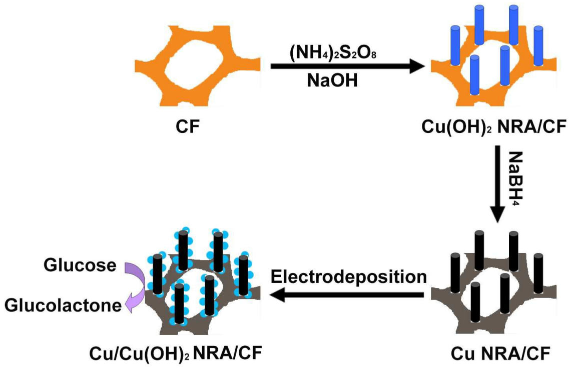

Scheme. 1 Three-step synthesis process for hierarchical $Cu/Cu(OH)_2$ NRA/CF and its application for glucose sensing.

View Article Online
DOI: 10.1039/C6RA19576H

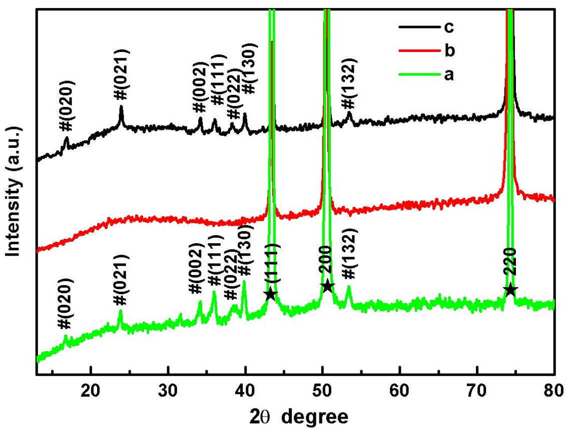

Fig. 1 XRD patterns of Cu(OH)$_2$ NRA/CF (curve a), Cu NRA/CF (curve b) and Cu/Cu(OH)$_2$ NRA/CF (curve c).

View Article Online
DOI: 10.1039/C6RA19576H

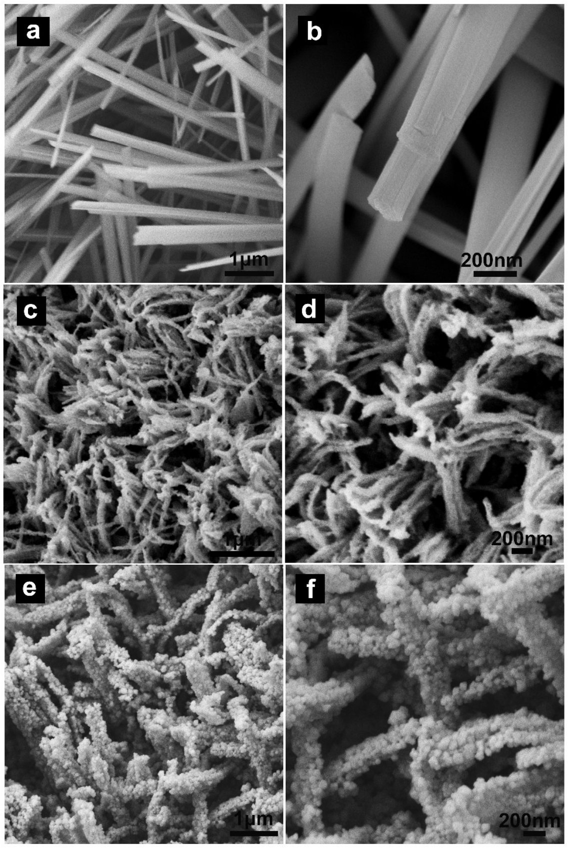

Fig. 2 Low and high-magnification SEM images of $Cu(OH)_2$ NRA/CF (a, b), Cu NRA/CF (c, d), and $Cu/Cu(OH)_2$ NRA/CF (e, f).

View Article Online
DOI: 10.1039/C6RA19576H

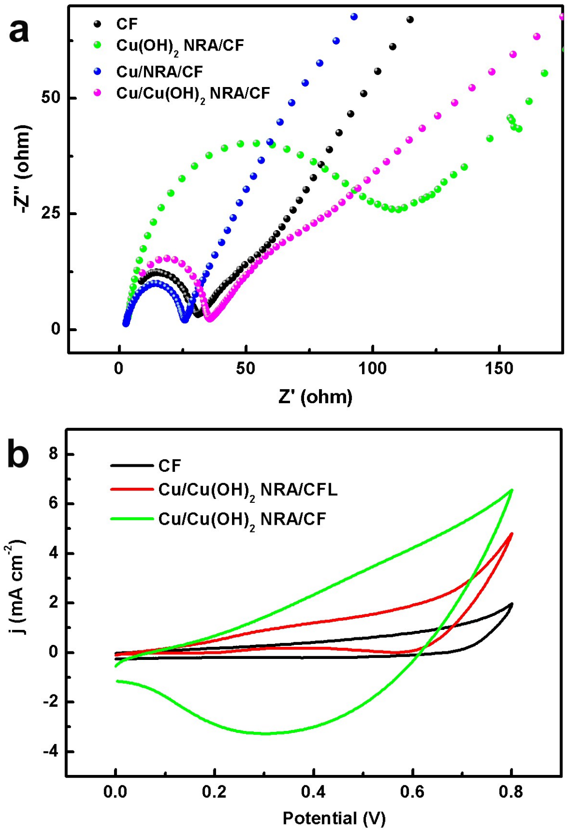

Fig. 3 (a). EIS results of CF, Cu(OH)$_2$ NRA/CF, Cu NRA/CF, and Cu/Cu(OH)$_2$ NRA/CF in 0.10 M KCl with the presence of 0.01 M equimolar [Fe(CN)$_6$]$^{3-/4-}$. (b). CVs of the CF, Cu/Cu(OH)$_2$ NRA/CF and Cu/Cu(OH)$_2$ NRA/CFL in 0.1 M NaOH solution with a scan rate of 20 mV/s.

View Article Online
DOI: 10.1039/C6RA19576H

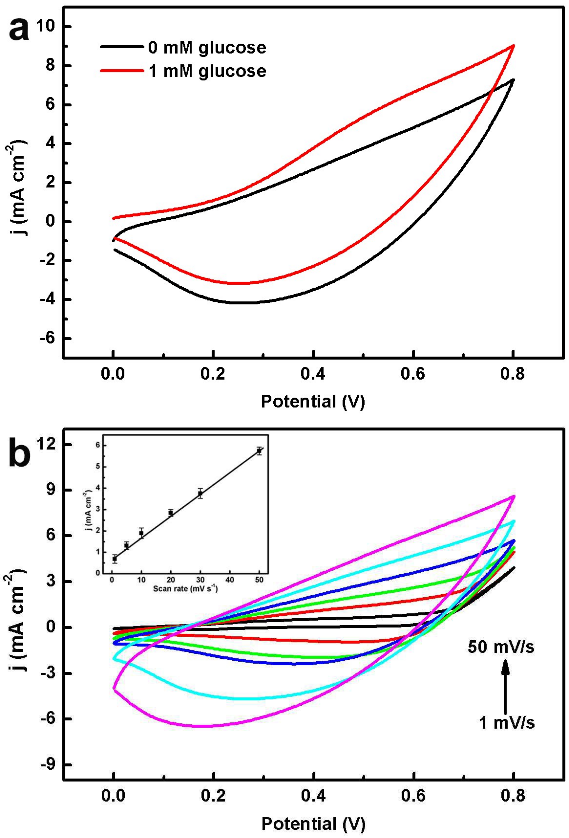

Fig 4. (a) CVs of Cu/Cu(OH)$_2$ NRA/CF in the absence (black curve) and presence (red curve) of glucose. (b) CVs of Cu/Cu(OH)$_2$ NRA/CF in 0.1 M NaOH at various scan rates of 1, 5, 10, 20, 30, 50 mV/s with the glucose concentration of 0.1 mM. Inset: the plot of the anodic response at 0.5 V vs. the scan rate.

View Article Online
DOI: 10.1039/C6RA19576H

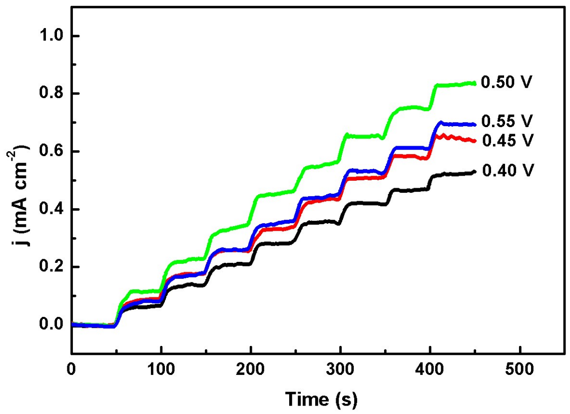

Fig. 5 Amperometric response with successive addition of 0.01 mM glucose at different detection potentials.

View Article Online
DOI: 10.1039/C6RA19576H

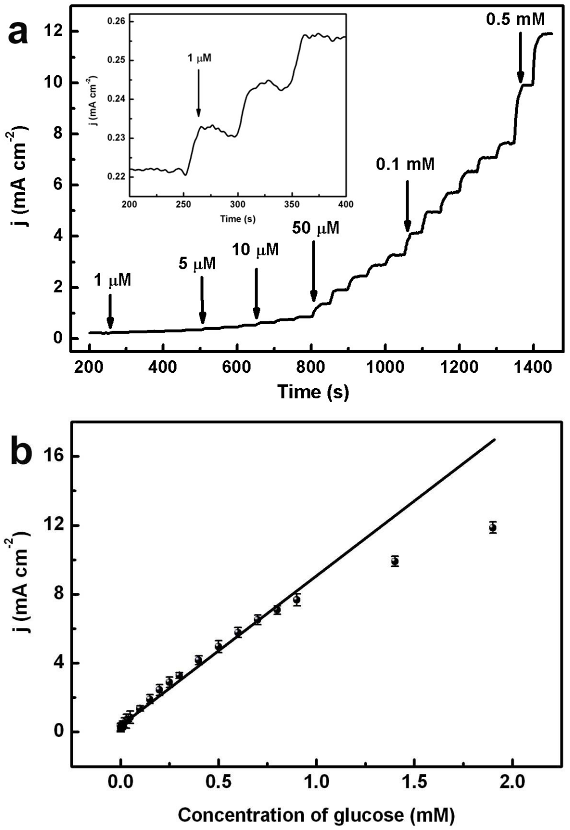

Fig. 6 (a) Amperometric response of Cu/Cu(OH)$_2$ NRA/CF with successive addition of the glucose solution of different concentrations into 0.1 M NaOH solution. Inset: enlarged amperometric response curve of the Cu/Cu(OH)$_2$ NRA/CF on addition of 1 μM glucose into NaOH solution. (b) Calibration curve for current vs. concentration of glucose.

View Article Online
DOI: 10.1039/C6RA19576H

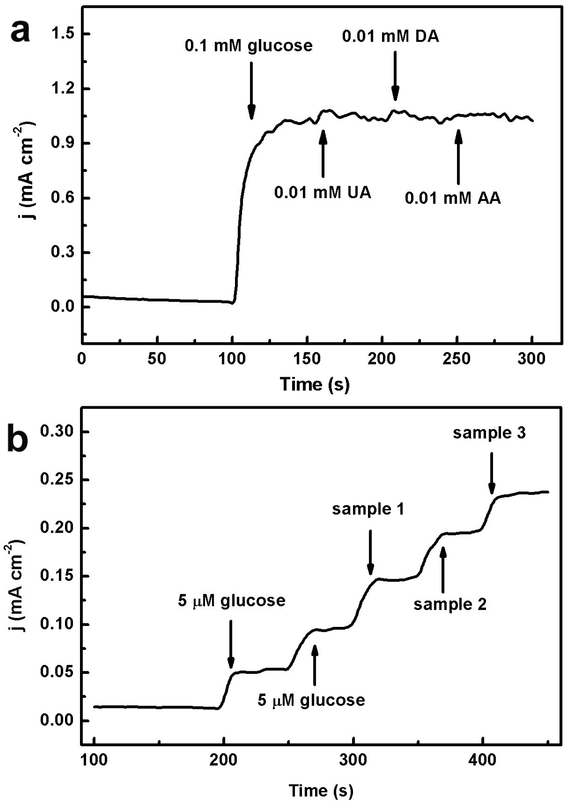

Fig. 7 (a). Amperometric response upon addition of 0.1 mM glucose, 0.01 mM UA, 0.01 mM DA and 0.01 mM AA at an applied potential of 0.5 V in 0.1 M NaOH solution. (b) Amperometric response upon addition of 5 μM glucose and three serum samples at an applied potential of 0.5 V in 0.1 M NaOH solution.

View Article Online
DOI: 10.1039/C6RA19576H

Table. 1 Glucose concentration in human serum samples that obtained in the hospital and those obtained by the $Cu/Cu(OH)_2$ NRA/CF sensor.

Sample	Glucose concentr-ation obtained from the hospital (mM)	Glucose concentra-tion obtained from the present sensor (mM)	RSD (%)	Bias (mM)
1	6.26	6.19	1.06	-0.07
2	5.75	5.87	2.29	0.12
3	4.73	4.83	2.45	0.10